Chaos, Solitons and Fractals 213 (2026) 119190

Contents lists available at ScienceDirect

Chaos, Solitons and Fractals

journal homepage: www.elsevier.com/locate/chaos

Dynamics of coupled nonlinear diffusion–reaction systems

Edward Larroza [a,b,*], Diego González [b,c], Sergio Curilef [c]

[a] Departamento de Física y Astronomía, Facultad de Ciencias Exactas, Universidad Andrés Bello, Sazié 2212, piso 7, Santiago, 8370136, Chile
[b] SMART INNOVA SpA, 14 de Febrero 2534, Of. 303, Ed. O'Brien, Antofagasta, 1240000, Chile
[c] Departamento de Física, Universidad Católica del Norte, Avenida Angamos 0610, Antofagasta, 1240000, Chile

ARTICLE INFO

Keywords:
Nonlinear dynamics
Anomalous diffusion
Reaction–diffusion systems
Reduced-order modeling
Emergent phenomena

ABSTRACT

We study two coupled nonlinear Fisher–Kolmogorov equations with anomalous diffusion. Because analytical solutions are difficult to obtain, we use a reduced collective-coordinate method based on two time-dependent power-law assumptions. This approach reduces the original partial differential equations to a simpler system of coupled ordinary differential equations that we can analyze semi-analytically. The simplified dynamics show two different populations. One of them follows logistic-like growth, described by an autonomous Bernoulli equation, and settles into a steady state. The other one grows quickly and reaches a point where the reduced model no longer works. By numerical methods, we solve the coupled nonlinear Fisher–Kolmogorov equations directly to compare both results. Our findings offer a simplified perspective on interacting nonlinear diffusion–reaction systems with unusual transport and nonlinear coupling. The comparison of the reduced system with the numerical results yields the interval of time where both solutions coincide. This approach provides a tractable route to study emergent dynamical structures in coupled nonlinear diffusion–reaction systems.

1. Introduction

Diffusion–reaction systems are widely studied because of their applications to transport and propagation processes in complex media. In particular, Fisher–Kolmogorov-like equations [1,2] are used to model front propagation, population dynamics, and collective phenomena in nonlinear diffusion processes competing with reaction mechanisms [3]. Recent studies have focused on anomalous diffusion, nonlinear transport, and nonlocal interactions, which go beyond the standard Gaussian description. Some nonlinear transport processes create distributions with either sharp cutoffs or heavy tails. In these cases, nonlinear Fokker–Planck [4,5] and Fisher–Kolmogorov (NFKE) [6–8] equations often lead to q-Gaussian distributions and unusual transport behaviors controlled by nonlinear diffusion with patterns in nonequilibrium and provide useful ways to approximate complex scaling and spreading effects. Complementary approaches based on fractional operators have also been developed for the asymptotic analysis of Fisher–KPP equations with anomalous diffusion [9], coupled neuronal dynamics supported by surrogate neural networks [10], and fractional epidemiological modeling [11].

Coupled NFKEs are typically difficult to solve analytically, and their numerical treatment is often computationally demanding. Consequently, reduced-order approaches based on collective coordinates [12–14], variational approximations [15,16], or effective-particle descriptions provide useful means to capture its dominant dynamical features.

Building on these considerations, we take a reduced collective-coordinate approach for a couple of NFKE with anomalous diffusion and nonlinear interactions. Our model is inspired by insect dispersal systems [17] used in mathematical biology, which

* Corresponding author at: Departamento de Física y Astronomía, Facultad de Ciencias Exactas, Universidad Andrés Bello, Sazié 2212, piso 7, Santiago, 8370136, Chile.
E-mail address: e.larrozahernandez@uandresbello.edu (E. Larroza).

https://doi.org/10.1016/j.chaos.2026.119190
Received 29 June 2026; Received in revised form 9 September 2026; Accepted 10 September 2026
0960-0779/© 2026 Elsevier Ltd. All rights are reserved, including those for text and data mining, AI training, and similar technologies.

we combine with the Plastino and Plastino equation [18] to formulate our proposal, considering anomalous diffusion and reaction terms. The following coupled NFKEs describe the interactions between two populations as follows:

$$\frac{\partial W}{\partial t} = \frac{\kappa}{2-q}\frac{\partial^2}{\partial x^2}W^{2-q} + rW - \mu V W^q, \tag{1}$$

$$\frac{\partial V}{\partial t} = \frac{\kappa'}{2-q'}\frac{\partial^2}{\partial x^2}V^{2-q'} + r'V - \mu\beta W V^{q'}, \tag{2}$$

where κ and κ' are the diffusion coefficients, r and r' stand for growth, and μ is the competition parameter that couples both equations. Instead of solving exactly for the entire set of equations, we approximate the evolving distributions using time-dependent q-Gaussian functions, characterized by their amplitudes, widths, and positions [18–20]. This method transforms the original complex system into a simpler, finite-dimensional one that allows us to track the evolution of these key parameters over time. By introducing the additional effective interaction kernel, β, the challenge is to handle the reduced system [21,22] while maintaining a nonlinear coupling structure consistent with the collective coordinate method.

The aim of this work is not to obtain exact analytical solutions of the NFKE system, but to identify a finite-dimensional approximately invariant manifold on which the dominant dynamics can be represented through collective coordinates by comparing with numerical resolution of the NFKE based in standard Crank–Nicolson method.

With this setup, the reduced equations show two main types of behavior. In one case, the system follows a logistic-like scaling pattern described by a Bernoulli equation. In the other, the system grows quickly as the reduced approximation loses accuracy. The time at which this breakdown occurs is determined by the collective coordinates diverging, not by a true singularity in the original equations.

The analysis identifies different behaviors in the parameter space, including long-lasting diffusion, intermediate scaling transitions, and rapid breakdowns of the reduced system. We characterize these behaviors using a combination of semi-analytical results and numerical calculations across the parameter space. This method provides a simpler way to study interacting nonlinear transport systems with unusual diffusion and nonlinear coupling. Beyond the specific model in this work, the approach could help analyze collective-coordinate reductions in many other nonlinear diffusion–reaction systems where exact solutions are difficult to obtain. Recent studies of nonlinear electrical networks have focused on compact-like pulse propagation in two dimensions [23], transverse stability and modulational instability of modulated waves [24], and exact and modulated compact solutions [25]. These results emphasize the importance of spatial localization and nonlinear wave evolution in coherent structure formation, providing a reduced description of evolving localized trends within the broader context of nonlinear transport, as investigated in the current work.

The remainder of this article is organized as follows: Section 2 provides an overview of the problem and defines the distributions of both populations studied using a couple of NLFKEs. Section 3 presents a dimensionless formulation of the equations and proposes a method for solving this type of equation using ansatzes based on power-law distributions to aid interpretation. Section 4 presents numerical results obtained directly from NFKE and discusses them from a diffusive perspective. We also present a dynamical phase diagram of the coupled NFKE system in dimensionless parameters related to the approximate dynamical structure. Section 5 introduces a possible application of the current formulation to economic populations related to workers and per capita income. Section 6 draws some concluding remarks.

2. Overview of the problem

As announced, we propose a model that generalizes a population that evolves and interacts with another static population [7] to two interacting populations that evolve according to two coupled NFKEs. The distributions involved in this problem are:

1. The distribution $W(x,t)$ represents a population that spreads and grows through the consumption of environmental resources.
2. The distribution $V(x,t)$ denotes another population, which spreads and grows independently of the previous, but consumes the same resources.

Using these definitions, we analyze interactions over time between populations, enabling us to identify the conditions under which stable, optimal distributions can emerge. At this stage, we choose two possible populations with the nonlinearity parameters $q = 2$ and $q' = 0$. Therefore, the set of two coupled NFKEs approaches a model of two interacting populations with asymmetric nonlinear coupling [17] as follows:

$$\frac{\partial W}{\partial t} = \kappa\frac{\partial^2}{\partial x^2}\log W + rW - \mu V W^2, \tag{3}$$

$$\frac{\partial V}{\partial t} = \frac{\kappa'}{2}\frac{\partial^2}{\partial x^2}V^2 + r'V - \mu\beta W, \tag{4}$$

where t is the time, after defining the model's functions and parameters, we propose using them in Eqs. (3) and (4) to construct the coupled NFKEs, and a function $\beta = \beta(x,t)$ to ensure closure of the semi-analytical approach, and make the interaction term consistent in a bounded form that agrees with the distribution $V(x,t)$, as discussed further.

The parameters $q = 2$ and $q' = 0$ are motivated by anomalous diffusive processes and analytical considerations. The nonlinearity of the logarithmic diffusion, $q = 2$, is associated with superdiffusive dynamics and large fluctuations [3], as occurs in continuity equations describing ionic concentrations, and corresponds to a superdiffusive regime characterized by heavy-tailed distributions. In contrast, the nonlinear term with $q' = 0$ yields a subdiffusive process, such as in porous media, with compact-support distributions associated with spatially confined systems [4], as the space distribution of a subdiffusive system of confined interacting particles with drag representing a population whose distribution has compact support. The values of q and q' correspond to opposite physical situations but are significant cases of anomalous diffusion.

3. Dimensionless analysis: Semi-analytical approach and numerical results

As mentioned above, the problem is difficult to discuss given the number of equations and parameters. However, to facilitate the analysis, let us write the set of Eqs. (3)–(4) in a dimensionless form. To identify the natural scales of the problem, we consider Eq. (3) in the limit where the reaction term dominates locally as a logistic equation, which allows us to introduce the following change of variables:

$$t = \frac{\tau}{r}, \quad x = \frac{\sqrt{\kappa\mu}}{r}\xi. \tag{5}$$

Using the notation

$$\frac{\partial}{\partial t} f = r\dot{f}, \qquad \frac{\partial^2}{\partial x^2} = \frac{r^2}{\kappa\mu}\partial_\xi^2,$$

and the proper distributions are:

$$W(x,t) = \frac{r}{\mu} w(\xi,\tau), \quad V(x,t) = v(\xi,\tau), \quad \beta(x,t) = b(\xi,\tau),$$

leading us to the set of the following dimensionless NFKE:

$$\dot{w}(\xi,\tau) = \partial_\xi^2 \log w(\xi,\tau) + w(\xi,\tau)(1 - v(\xi,\tau)w(\xi,\tau)), \tag{6}$$

$$\dot{v}(\xi,\tau) = \frac{K}{2}\,\partial_\xi^2 v(\xi,\tau)^2 + Rv(\xi,\tau) - b(\xi,\tau)\,w(\xi,\tau), \tag{7}$$

where the Eq. (6) is invariant under scaling because of the logarithmic diffusion, and it is free of parameters. Eq. (7) depends on the parameters:

$$K = \frac{\kappa' r}{\kappa\,\mu}. \quad R = \frac{r'}{r}, \tag{8}$$

This choice reduces the five original parameters to only two effective dimensionless parameters.

In relation to Eq. (7), we define the effective interaction field $\mathcal{L}(\xi,\tau)$ by $\mathcal{L} = bw$, and equivalently $b = \mathcal{L}/w$. This interpretation is useful because it separates the normalized spatial distribution of the interaction from its coupling to the field w. If, in addition, we impose a partial regulation-like mechanism [26] on the distribution $v(\xi,\tau)$, we rephrase it as

$$\dot{v}(\xi,\tau) = \frac{K}{2}\,\partial_\xi^2 v(\xi,\tau)^2 + Rv(\xi,\tau) - \mathcal{L}(\xi,\tau), \tag{9}$$

to control the population v size across a spatial area, independently of local parameter fluctuations. This is proposed by the normalization condition

$$\int_{\xi_{\min}(\tau)}^{\xi_{\max}(\tau)} v(\xi,\tau)\,d\xi = 1, \qquad \text{and} \qquad v(\xi,\tau) \geq 0, \tag{10}$$

where $\xi_{\min}$ and $\xi_{\max}(\tau)$ define the outer boundaries of a time-dependent region where v has compact support. From this condition, integrating Eq. (7), we get

$$R = \int_{\xi_{\min}(\tau)}^{\xi_{\max}(\tau)} \mathcal{L}(\xi,\tau)d\xi, \tag{11}$$

with $\mathcal{L}(\xi,\tau) = \mathcal{L}_0(\tau) + \mathcal{L}_1(\tau)\big(\xi - \xi_p(\tau)\big)$ where $\mathcal{L}_0(\tau)$ is the relevant term of the regularization condition, corresponding to the lowest-order ξ-dependence and whose integral over ξ vanishes. It is centered at $\xi_p(\tau)$, as $v(\xi,\tau)$ is centered as well. The integral is performed over the same domain defined by conditions (10). Here we adopt a parabolic form for the initial condition distribution. It is not introduced as an empirical approximation, but is a polynomial closure of the nonlinear diffusion term together with the lowest spatial form of the regulation term. We consider

$$v(\xi,\tau) = g_1(\tau) - g_2(\tau)\big(\xi - \xi_p(\tau)\big)^2, \tag{12}$$

$$v^2 = g_1^2 - 2g_1g_2\big(\xi - \xi_p(\tau)\big)^2 + g_2^2\big(\xi - \xi_p(\tau)\big)^4, \tag{13}$$

where $g_1 > 0$ and $g_2 > 0$, therefore $v(\xi,\tau)$ and $\partial_\xi^2 v^2$ are the same order in $\xi - \xi_p(\tau)$. This observation identifies a finite-dimensional invariant manifold of the PDE. For the effective interaction term $\mathcal{L}$, we take the lowest-order nontrivial form

$$\mathcal{L}(\xi,\tau) = \mathcal{L}_0(\tau) - m(\tau)\left[\xi - \xi_p(\tau)\right]. \tag{14}$$

where $m(\tau)$ is a time coefficient to express the coupling $b(\xi,\tau)$, and from the auxiliary function (14) in combination with Eq. (12), we obtain $\mathcal{L}_0(\tau) = \dfrac{2R}{3}g_1(\tau)$. Now, considering the definition (12) and imposing the same regulation condition of the Eq. (10) to obtain the auxiliary relationship between g_1 and g_2

$$g_1(\tau) = \left(\frac{3}{4}\right)^{2/3} g_2(\tau)^{1/3}. \tag{15}$$

where $g_1(\tau)$ is the amplitude of the distributions $v(\xi,\tau)$; while $\xi_p(\tau)$ is its mode. So far, we have analyzed the general properties of NFKEs (9) to show that the parabolic distributions (12) define an invariant solution manifold.

Solutions of the NFKEs system (6) and (7) are approximated using the ansatzes of the q-Gaussian type, specifically considering the 2-Gaussian and 0-Gaussian cases. Therefore, the ansatzes that solve the equations are:

$$w(\xi,\tau) = \left(a(t) + \frac{[\xi-\zeta(\tau)]^2}{4s(\tau)}\right)^{-1}, \tag{16}$$

$$v(\xi,\tau) = \left[g_1(\tau) - g_2(\tau)\left(\xi-\xi_p(\tau)\right)^2\right]_+, \tag{17}$$

where Eq. (17) rephrases Eq. (12) for the distribution $v(\xi,\tau)$ with the notation $[\mathcal{A}]_+$ indicating that only real and positive values of $\mathcal{A}$ are considered. The current semi-analytical approach is based on a collective-coordinate reduction of the coupled NFKE. Instead of solving the full NPDE dynamics, the evolution is restricted to a reduced manifold parametrized by amplitudes, widths, and modal positions associated with q-Gaussian distributions. Within this framework, the ansatzes (16) and (17), because the nonlinear interaction terms do not preserve exact invariance of this manifold under the full NPDE flow, we introduce the auxiliary field $b(\xi,\tau)$, which acts as an effective closure kernel. Its function is to maintain compatibility between the nonlinear coupling structure and the reduced collective-coordinate dynamics, thereby preserving analytical tractability. More specifically, the interaction field $b(\xi,\tau)$ is a kind of conditional probability related to the state $w(\xi,\tau)$. Therefore, $b(\xi,\tau)d\xi$ stands for the conditional probability within the interval $d\xi$.

The resulting ordinary differential equations system should be interpreted as a reduced collective-coordinate approximation rather than an exact invariant reduction of the original NFKE.

An assessment of the $b(\xi,\tau)$ and the explicit relationship with $m(\tau)$ is discussed in B. This parameter is interpreted as a weight that modulates the effectiveness of $w(\xi,\tau)$ in different regions of space and time through coupling. It sets a global interaction scale by influencing the displacement of the mode of $v(\xi,\tau)$.

Therefore, the two coupled NFKEs can be rephrased as a set of coupled ordinary differential equations for the variables $(a,\zeta,s,g_1,g_2,\xi_p,m)$ and (b,w,v) which are functions of time and space and time, respectively. Hereafter, for simplicity, the explicit dependence on time will be omitted. Thus, the set of equations of motion reads:

$$\dot{a} = \frac{a}{2s} - a + g_1 - g_2\,(\zeta-\xi_p)^2, \tag{18}$$

$$\dot{\zeta} = 4g_2\,(\zeta-\xi_p)s, \tag{19}$$

$$\dot{s} = \frac{1}{2} + s + 4g_2 s^2, \tag{20}$$

$$\dot{g}_2 = -6\,K\,g_2^2 + R\,g_2, \tag{21}$$

$$\dot{\xi}_p = \frac{m}{2g_2}. \tag{22}$$

This work is performed from Eqs. (18)–(22) together with the auxiliary condition (15). As observed, equations of motion are derived from the two nonlinear and coupled differential equations that control the dynamics and interactions of our system, and some details of the derivation of the previous set of equations are given in the A. The usefulness of the coupling coefficient b is mathematically well justified because it allows the construction of a set of ordinary differential Eqs. (18)–(22), easier to handle and solve analytically and numerically. Also, we note that Eq. (20) is a Riccati equation and Eq. (21) is called as autonomous Bernoulli equation of degree 2.

By classifying these equations, we guarantee that the set of Eqs. (18)–(22) can be solved analytically; however, we prefer a semi-analytical (numerical) approach. Solving nonlinear partial differential equations (NPDE) generally requires intensive numerical work and substantial computational resources. Nevertheless, in this contribution, we have presented semi-analytical solutions for NFKE concluding the work through numerical development.

In addition, proving the existence and uniqueness of solutions to NPDE is a nontrivial challenge and is usually very difficult. A discussion of these issues is beyond the scope of this work. In consequence, the solutions are valid under the assumption that, on the one hand, the initial condition takes the form of a Lorentzian given by $\left(a_0+(\xi-\zeta_0)^2/(4s_0)\right)^{-1}$ that is centered at ζ_0 of the coordinates, where a_0^{-1} is the amplitude of the pulse w and $\sqrt{s_0\,a_0}$ is proportional to the initial width of the pulse, and on the other hand, the parabola $(g_{10} - g_{20}\,(\xi-\xi_{p0})^2)$ is centered at ξ_{p0} of coordinates where g_{10} is the initial amplitude and the initial width of the parabola is proportional to $\sqrt{g_{10}/g_{20}}$. The initial g_{10} and g_{20} are also combined by Eq. (15).

4. Diffusive behavior

The evolution of the distribution w is characterized by heavy tails, in contrast to v, which is a distribution with compact support.

The evolution of the distribution exhibits nontrivial diffusive behavior, which needs to be defined on a finite data interval, since the second moment of the variable ξ is not defined in all space. However, to avoid this, we prefer to use the Half-Width at Half-Maximum (HWHM) as an indicator of anomalous diffusion behavior, defined as the distance between the maximum and the point at which the distribution reaches half of its maximum values. Since diffusion is related to the dispersion of the distribution, a suitable indicator is

$$\gamma_w = \mathrm{HWHM}_w^2 = s\;a \tag{23}$$

Indeed, the diffusion is anomalous, and we need to determine the typical behavior that is expected for several values of the parameters R and K.

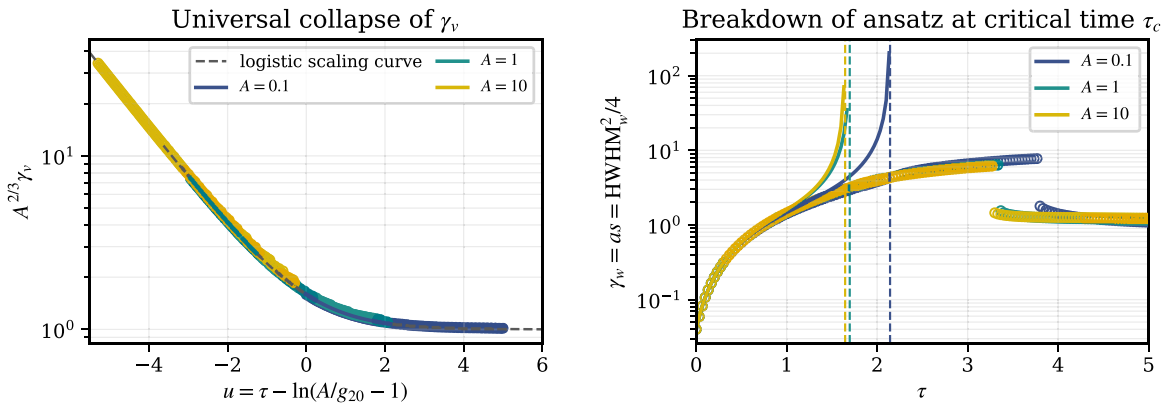


Fig. 1. (*a*) The observable $\gamma_v = g_2^{-2/3}$ exhibits a scaling collapse of the manifold approximation under the transformation $u = \tau - \ln(A/g_2(0) - 1)$, where $A = R/6K$ and $R = 1$. In contrast, (*b*) $\gamma_w = as$ does not exhibit the same scaling collapse, and instead develops a strong growth toward a finite critical time τ_c, denoting the range of validity of the ansatz. Solid lines represent solutions from the ansatz, and circles represent direct numerical solutions of the NFKE system.

Unlike the previous case, the second moment of ξ is well defined by the variance, therefore

$$\gamma_v = \frac{1}{2}\left(\frac{3}{4}\right)^{2/3} g_2^{-2/3}, \tag{24}$$

which allows the establishment of a diffusion law. In all cases, the system exhibits anomalous diffusion. In all cases, both γ_v and γ_w are not proportional to τ.

As depicted in Fig. 1a, the γ_v decreases as τ increases. Eq. (21) is a nonlinear ordinary differential equation with constant coefficients, and has a typical logistic-like solution g_2 that does not depend on the dynamics of the other population. At small times, the growth is exponential, and the parameter R determines the rate of increase.

The reduced parameter $A = \dfrac{R}{6K}$ denotes a stable equilibrium value, namely if $\tau \to \infty$, then $g_2 \to A$.

To represent in a simple universal form, we define the natural effective length as $\sim \sqrt{\gamma_v}$, where the universal form and the observable γ_v can be given by

$$\Phi(u) = \left[1 + e^{-u}\right]^{1/3} \quad \Longrightarrow \quad \gamma_v = A^{-2/3}|\Phi(u)|^2 \tag{25}$$

where $u = \tau - \ln\left(A/g_2(0) - 1\right)$, with $A > g_2$, acts as invariant scaling factor for $R = 1$. This form is universal because the behavior at long times does not depend on the details of the microscopy.

According to this variable, the dynamics of γ_v is governed by a single effective scale generated by the logistic flow of g_2. In general, the autonomous Bernoulli equation governs a flow that converge toward a single stable attractor. Sometimes, a suitable variable change reduces the solution to $\Phi(u)$, which is then presented in various more complex contexts as the solution.

For finite values of the parameter A, the system reveals finite variance within a confined dynamical regime, whereas the flux evolves toward an exponential contraction regime for $A \to \infty$. The exponent $2/3$ emerges as an effective scaling exponent associated with the universal collapse of γ_v. Consequently, the scaling law $A^{2/3}\gamma_v$ removes the explicit dependence on A, mapping the dynamics onto the invariant scaling function $\Phi(u)$, consistent with a stable single-parameter flow.

We compared the collective-coordinate solution for γ_v with a direct Crank–Nicolson integration of the regulated NKFE system, fixing $K = R/6A$ with $R = 1$ and $A = 0.1, 1, 10$, and using initial conditions $g_{20} = 0.05$ and $m = 0$. The relative difference is less than 1%, and visually it is not possible to distinguish any discrepancy between lines (ansatz) and circles (Crank–Nicolson). Fig. 1a shows the coincidence of the collapsing curves.

The second population is governed by the Riccati Eq. (20), associated with the observable

$$\gamma_w = as,$$

which does not satisfy the same scaling law as γ_v. Its dynamics is dominated by the nonlinear growth of $s(\tau)$, which evolves toward a finite-time critical timescale τ_c, as shown in Fig. 1b). While γ_v exhibits a universal diffusive scaling collapse associated with the logistic flow of g_2, the observable γ_w displays a non-universal dynamical instability connected to the progressive loss of validity of the reduced collective-coordinate manifold. In particular, g_2 approaches a large-scale flow, whereas the rapid growth of $s(\tau)$ signals the breakdown of the reduced q-Gaussian approximation.

Accordingly, the observable $\gamma_w = as$ grows rapidly as $\tau \to \tau_c$ due to the divergence of the collective coordinate $s(\tau)$. Although it indicates a progressive loss of validity of the reduced collective-coordinate approximation, this behavior should not be interpreted as a true singularity of the original NPDE system. The divergence is better understood as a breakdown of the ansatz closure rather than as a rigorous singularity formation in the full coupled NFKE dynamics.

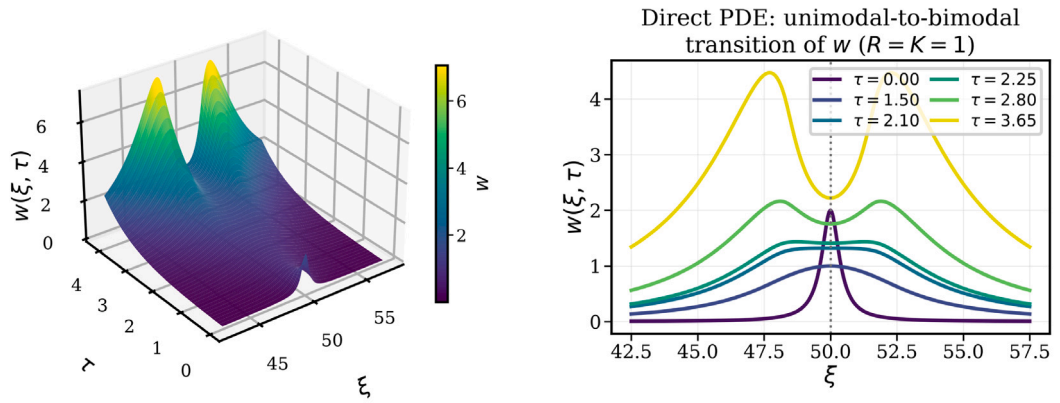


Fig. 2. The numerical solution $w(\xi,\tau)$ of the NFKE (7) is depicted in (a) as a function of ξ and τ. Panel (b) depicts the distribution as a functions of ξ for τ fixed at 0, 1.5, 2.1, 2.25, 2.8, and 3.85. It is notorious the change from unimodal to bimodal at $\tau \approx 2.1$. Parameters $R = K = 1$, namely $A = 1/6$.

Fig. 1b $\gamma_w = as = \mathrm{HWHM}_w^2$ shows that both methods agree during the early evolution: for $\tau < \tau_c/2$, the worst root-mean-square and pointwise square errors are 1.65% and 4.79%, respectively. Nevertheless, close to τ_c, the Lorentzian width diverges; the numerical NFKE solution remains finite and subsequently develops a bimodal profile. The main reason why the ansatz produces a breakdown at τ_c, shown in Fig. 1b, is that the Lorentzian distributions do not correspond to an invariant solution manifold.

Fig. 2 shows how the numerical solution evolves from an unimodal distribution (Lorentzian) toward a bimodal one. The distribution shows long tails on both sides of the solution, compatible with a Lorentzian in early evolution. However, at $\tau \approx 2.1$, a plateau is observed in the center of the solution, forming a bimodal distribution for $\tau > 2.1$. The present results, therefore, characterize the dynamical stability of the reduced manifold rather than the complete regularity properties of the initial NFKE system. The breakdown appearance, which is shown in Fig. 2, defines the interval of τ where the ansatz is valid. As τ approaches τ_c, the evolution based on the ansatz that represents w departs from the exact numerical solution obtained from the NFKE, and the discontinuity observed in the numerical solutions (circles) is due to the change from unimodal to bimodal, where γ_w needs to be assessed, modifying the strategy. But this is not an objective of the current paper.

The distributions for Figs. 1 and 2 were calculated on $0 \le \xi \le 100$, with the center of the initial profile translated to $\xi_0 = 50$ to keep it far from the boundaries; the final times were $\tau = 5$ and 6.5, respectively. The nonlinear residual tolerance for the calculation of v is 10^{-10}, and the coupled-iteration tolerance is set to 2×10^{-8} for the convergence of the self-consistent solution of the coupled w and v system.

Fig. 3 shows an approximate dynamical phase diagram of the coupled NFKE system for the critical time τ_c in color scale in the dimensionless parameter plane (R, K). The map of Fig. 3 depicts the intricate dynamics of competition between the nonlinear diffusion and reaction mechanisms.

The approximate topology in the (R, K) plane can be summarized as

- **Red region (Short-lived):** Characterized by small critical times ($\tau_c \ll 1$), this zone represents a regime dominated by a rapid finite-time instability where the ansatz quickly breaks down.
- **Yellow region (Intermediate):** Acting as the intermediate domain, this region accommodates the gradual transition between the long-lived and short-lived phases.
- **Blue region (Long-lived):** Long-lived transient and diffusive regimes are observed, where the cooperative effects significantly delay the breakdown of the reduced dynamics, extending the system's lifetime.

Thresholds of the reduced parameter ($A \sim 1$), which formally demarcates the balanced competition where the logistic regularizing flow of the first population matches the destabilizing rate of the second. If $\tau_c \gg 1$, the Lorentzian ansatz evolves delaying its change of shape where its amplitude is so great ($a \to 0$) and s also increases. This phenomena it is demarked by a discontinuous white line in Fig. 3.

5. Socio-economic application

This analysis focuses on socio-economic systems instead of biological ones. It looks at populations that both collaborate and compete. The solutions are distributions understood through population dynamics. The framework gives a way to measure how macroeconomic shocks, inequality, and debt policies affect income changes and social views. This model suggests that crises are shaped by changes in several economic indicators, not just by their timing. Using nonlinear diffusion and stability analysis, the model shows how dissatisfaction and instability can develop in economies facing structural challenges.

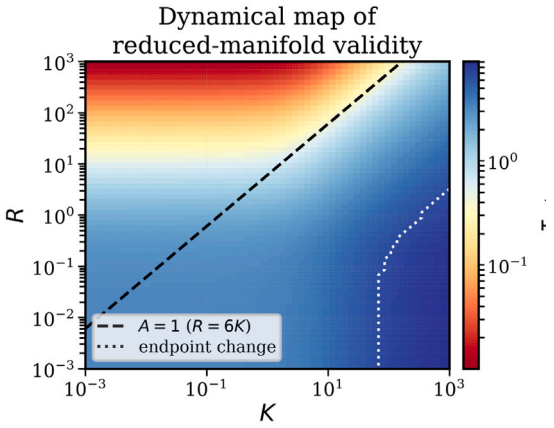


Fig. 3. We depict three different dynamical sectors: a diffusive regime dominated by slow evolution, a crossover region displaying scaling behavior, and a finite-time instability produced by the ansatz sector characterized by rapid divergence and breakdown emphasizing where the ansatz fails.

The current model builds on earlier work that described a single population changing over time with macroeconomic factors using a single NFKE [6]. Now, it considers two interacting populations, modeled with two coupled NFKEs, similar to diffusion–reaction systems like Eqs. (6) and (7), solved in the same numerical and semi-analytical ways. These populations are not like the usual predator–prey models, but instead are defined as follows:

1. The distribution $w(\xi,\tau)$ shows the density of per-capita economic capacity. This group considers families with children, people out of work, or those who contribute little to family income. All share household responsibilities.
2. The distribution $v(\xi,\tau)$ refers to net income-generating workers, including only working-age people who earn a net income in the country.

The space (ξ,τ) uses an economic coordinate ξ scaled by 10^5 CLP (Chilean pesos) for income level and a time coordinate τ (time in years) for measuring how things change over time. The term bw measures the economic burden on those who generate income. We define an adaptive vulnerability field [27] as $b = \mathcal{L}/w$, where $\mathcal{L}$ shows how the burden is spread out. This means the main interaction depends on the product $bw = \mathcal{L}$, not just the income level w. In this model, $\mathcal{L} = \frac{2}{3}Rg_1 - m(\tau)(\xi - \xi_p)$, where $m(\tau) = -\partial_\xi \mathcal{L}$ is the gradient of economic burden and $\xi_p(\tau)$ marks its main socioeconomic location. This shows how the working population moves, which can be used as another useful indicator because it tracks the peak of worker income. If $m = 0$, vulnerability is the same everywhere. If $m > 0$, vulnerability goes down as ξ increases. If $m < 0$, vulnerability goes up as ξ increases. This can become a measurable socioeconomic value if ξ is defined appropriately. Another useful measure is $\gamma_v(t)$, which shows how spread out the working population is.

With this approach, we study how net income distribution and per capita spending patterns interact over time in the income space. This helps us find the conditions that lead to stable and optimal economic distributions. Beyond any detail of employees and family income distributions, let us consider the following initial conditions:

$$w(\xi,0) = \frac{0.272}{1 + 0.446 \times (\xi - 1.83)^2}, \tag{26}$$

$$v(\xi,0) = 0.2 - 1.42 \times 10^{-2}(\xi - 4.8)^2, \tag{27}$$

We remark that $w(\xi,0)$ fitted by Eq. (26) is inspired by the empirical data of the classification that Chile makes of the social level. The "deciles" refer to the method used to measure family income in Chile, which is applied to determine eligibility for free tuition and other student benefits, dividing the population into 10 equal-sized groups (deciles). If their households are located in the 50%–60% lowest deciles, they may be eligible, provided that they meet the other requirements and that their institution is eligible for this benefit. Additionally, the distribution $v(\xi,0)$ given by Eq. (27) evokes the real case related to a given country, like Chile. The initial distribution $v(\xi,0)$ is expressed approximately through (27), where the amplitude coincides with the empirical amplitude: 20% of the population has an average net income given by 4.8×10^5 CLP, corresponding to a value close to the Chilean minimum income.

We expect the current model can capture the economic dynamics of the Chilean population because several specialists and politicians propose imposing a minimum and maximum employee income described by the distribution v with compact support. The distribution w fits family income across deciles and displays a heavy tail [28], like a Lorentzian. It is plausible to assume that the family income can be described by this solution before changing the shape while remaining unimodal. This economic distribution is certainly not bimodal. Regarding parameters R and K, they are close to 1 because they are ratios of comparable economic measures of income growth.

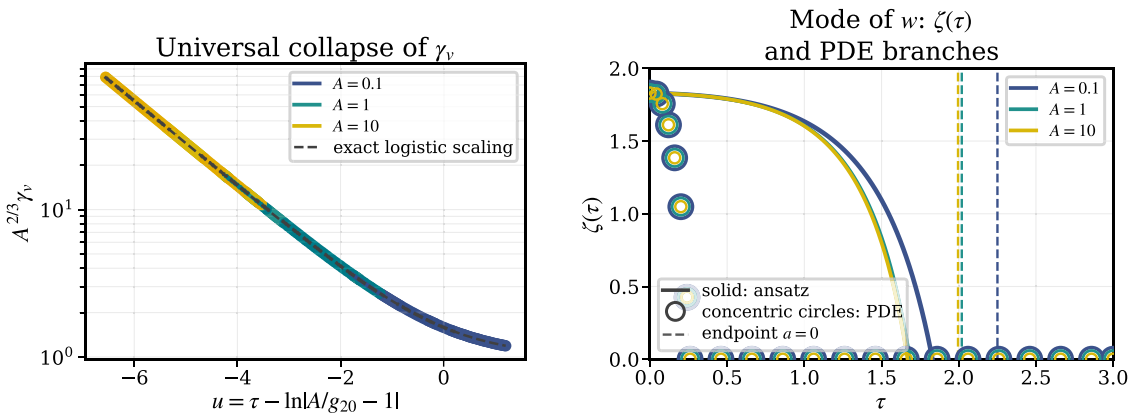


Fig. 4. (a) The scaled width $A^{2/3}\gamma_v$ is depicted to highlight the collapsing law. (b) The mode evolution of the distribution w is shown as possible relevant indicator of family income mobility. The initial profiles are displayed for $0 \leq \xi \leq \ell = 50$, evolving up to $\tau = 3$.

We remark in Fig. 4a the collapse of the width according the same law $A^{2/3}\gamma_v$ for different values $A = 0.1,\ 1$, and 10. Fig. 4b shows the mode dynamics of the distribution w as an indicator of family income mobility, with various increasing parameters held at the same values of A. The evolution of the variable leads the variable $\zeta(\tau)$ to *zero*. This indicates that the population that does not contribute to the per-capita family income increases ($1/a \to \infty$), this fact makes that the per-capita income decreases $\zeta \to 0$. Previous studies have suggested this indicator as a mediating variable linked to the causes of social conflict, such as declining citizen trust, state anxiety, lower perceived social status, and lower subjective well-being [6,29].

6. Concluding remarks

This study investigates the approximate dynamical phases of two populations modeled by two coupled NFKE. Two coupled nonlinear partial differential equations are reduced to a semi-analytical tractable system of five ordinary differential equations. We introduce a coefficient that depends on the inverse of the predator-like population density to capture an effective nonlinear interaction structure, and by applying saturated coupling to construct a tractable reduced-order collective-coordinate description. We use a global regulation mechanism to maintain the stability of a one of populations, imposing a constant normalization, while capturing fluctuations in the distribution's components through the dynamics of its width and height. The ansatzes are inspired by q-Gaussian distributions associated with nonextensive statistical mechanics. The advantage of this procedure is that a set of ordinary differential equations tracks the evolution of the coefficients. This semi-analytical approach allows us to describe and identify the competition process that emerges after solving the equation set, up to an instability threshold beyond which the ansatz breaks down.

The main finding reveals a dual dynamical behavior. Clear differences are observed between the two systems. One collective coordinate follows an autonomous Bernoulli equation that exhibits a universal contraction toward a stable asymptotic flow. An invariant scaling transformation ensures that all trajectories converge to a single point, regardless of the initial conditions. In this regime, the scaling exponent appears to serve as an effective exponent, characterizing the anomalous scaling dimension that reduces sensitivity to parameter-dependent transient dynamics. The second dynamics is governed by the Riccati equation, whose solutions yield non-universal dynamical behavior that does not scale as the first does. The system is driven by a diffusive mechanism toward a finite-time loss of validity $\tau \to \tau_c^-$ through the divergence $(\tau - \tau_c)^{-1}$. This behavior indicates whether the ansatzes are valid; in turn, that an emerging progressive departure from the reduced collective-coordinate manifold is occurring.

The dynamical diagram shown in Fig. 3 should therefore be interpreted as a map of the validity of the reduced-order description rather than a phase diagram of the original NKFE system. As described, the smooth dynamical crossover is represented in a (R, K) parametric plane. A dashed line in $R \sim 6$ K or equivalently $A \sim 1$ shows the balance between the nonlinear diffusion and reaction mechanisms. The map distinguishes at least three regions, red region of short-lived, yellow region for intermediate-lived, and blue region for long-lived.

Numerical verification of the reduced collective-coordinate approximation offers us a practical approach to coupled transport phenomena in complex environments; when applied to socio-economic dynamics, it shows that coupled NFKEs can capture the interactions between per-capita economic capacity and income-generating populations, providing a quantitative tool to track income mobility and structural vulnerabilities.

Future research could examine how external stochastic fluctuations or environmental symmetry breaking affect asymptotic logistic-like dynamics, or whether analogous scaling exponents exist in higher-dimensional multispecies systems. Such approximations can contribute to a better understanding of reduced-order descriptions of interacting nonlinear transport systems. Furthermore, while $b(\xi, \tau)$ provides an analytical closure to enforce manifold invariance, future developments could leverage data-driven order-reduction frameworks — such as Physics-Informed Neural Networks (PINNs) or Neural ODEs — to learn the effective interaction kernel directly from full PDE spatiotemporal data without a priori algebraic closures.

CRediT authorship contribution statement

Edward Larroza: Writing – original draft, Methodology, Conceptualization. **Diego González:** Software, Investigation, Data curation. **Sergio Curilef:** Writing – review & editing, Methodology, Conceptualization.

Declaration of competing interest

The authors declare that they have no known competing financial interests or personal relationships that could have appeared to influence the work reported in this paper.

Acknowledgments

We acknowledge FONDEF-ANID-SUC250298 and FONDECYT 1240810 for partial financial support, and Núcleo de Investigación No. 2 UCN-VRIDT 042/2020 "Sistemas Complejos en Ciencia e Ingeniería" for the technical and logistical contributions to this research.

Appendix A. Derivation of the set of nonlinear first-order differential equations

Writing explicitly every term of Eq. (7) using the ansatz (16), we get to:

$$\dot{w} = -w^2\left[\dot{a} - \frac{(\xi-\zeta)^2}{4s^2}\dot{s} + \frac{(\xi-\zeta)\dot{\zeta}}{2s}\right], \tag{28}$$

$$\frac{\partial^2 \log w}{\partial \xi^2} = -w^2\left[\frac{a}{2s} + \frac{(\xi-\zeta)^2}{8s^2}\right], \tag{29}$$

$$w = w^2\left[a + \frac{(\xi-\zeta)^2}{4s(\tau)}\right], \tag{30}$$

$$vw^2 = w^2\left[g_1 - g_2\left(\xi^2 + 2(\zeta-\xi_p)\xi + \zeta - \xi_p\right)^2\right], \tag{31}$$

where $\xi - \xi_p = (\xi-\zeta) + (\zeta-\xi_p)$ is applied to Eq. (31), to substitute in Eq. (7). This replacement yields

$$-\dot{a} + \frac{(\xi-\zeta)^2}{4s^2}\dot{s} + \frac{\xi-\zeta}{2s}\dot{\zeta} = -\frac{a}{2s} + ra - g_1 + g_2(\zeta-\xi_p)^2 + (\xi-\zeta)^2\left(\frac{1}{8s^2} + \frac{r}{4s} + g_2\right) + 2g_2(\xi-\zeta)(\zeta-\xi_p).$$

Identifying like terms, we obtain the first set of differential equations of first order

$$\dot{a} = \frac{a}{2s} - a + g_1 - g_2(\zeta-\xi_p)^2, \tag{32}$$

$$\dot{\zeta} = 4g_2(\zeta-\xi_p)s, \tag{33}$$

$$\dot{s} = \frac{1}{2} + rs + 4g_2 s^2, \tag{34}$$

As previously written, the terms of the Eq. (4) using the ansatz (17) are given by

$$\dot{v} = \dot{g}_1 - \dot{g}_2(\xi-\xi_p)^2 + 2g_2\dot{\xi}_p(\xi-\xi_p), \tag{35}$$

$$\frac{\partial^2}{\partial\xi^2}v^2 = 12g_2^2(\xi-\xi_p)^2 - 4g_1g_2, \tag{36}$$

$$v = g_1 - g_2(\xi-\xi_p)^2, \tag{37}$$

$$bw = \frac{2}{3}Rg_1 - (\xi-\xi_p)\,m. \tag{38}$$

The explicit dependence between b and m is shown in the B. With all this in mind, we obtain the equation.

$$\dot{g}_1 - \dot{g}_2(\xi-\xi_p)^2 + 2g_2(\xi-\xi_p)\dot{\xi}_p = 2Kg_1g_2 + Rg_1 - \frac{2}{3}Rg_1 + (\xi-\xi_p)^2\left(6Kg_2^2 - Rg_2\right) + (\xi-\xi_p)m.$$

Again, we identify like terms to arrive at the following set of differential equations of first order

$$\dot{g}_1 = -2Kg_1g_2 + Rg_1 - \frac{2}{3}Rg_1, = \frac{1}{3}g_1\left(-6Kg_2 + R\right) = \frac{1}{3}\frac{g_1}{g_2}\dot{g}_2 \tag{39}$$

$$\dot{\xi}_p = \frac{m}{2g_2}, \tag{40}$$

$$\dot{g}_2 = -6Kg_2^2 + Rg_2. \tag{41}$$

Thus, Eqs. (32)–(34) and (39)–(41) correspond to the entire set of differential equations of first order, which is reduced to five by applying the regulation-like mechanism of the Eq. (10), leading to the set of Eqs. (18)–(22) that we need to solve instead of the NPDE given by Eqs. (6) and (7).

Appendix B. Relationship between $b(\xi,\tau)$ and $m(\tau)$

The relation $b(\xi,\tau)d\xi$ represents the conditional probability of an interaction occurring within the interval $d\xi$, given the state of the w-field. We have imposed that

$$b(\xi,\tau)=\frac{\frac{2}{3}Rg_1-m\ (\xi-\xi_p)}{w(\xi,\tau)}, \tag{42}$$

and satisfies the normalization condition

$$\int_0^{\ell} d\xi\ b=1. \tag{43}$$

We lead the integral, satisfying the normalization condition (43), into two relevant integrals:

$$\frac{2}{3}Rg_1 I_1-m\ I_2=1, \tag{44}$$

where

$$I_1=\int_0^{\ell}\left(a+\frac{(\xi-\zeta)^2}{4s}\right)d\xi, \tag{45}$$

$$I_2=\int_0^{\ell}(\xi-\xi_p)\left(a+\frac{(\xi-\zeta)^2}{4s}\right)d\xi. \tag{46}$$

We get

$$I_1=a\ell+\frac{(\ell-\zeta)^3+\zeta^3}{12s}. \tag{47}$$

$$I_2=a\left(\frac{\ell^2}{2}-\xi_p\ell\right)+\frac{1}{4s}\left[\frac{\ell^4}{4}-\frac{2\zeta}{3}\ell^3+\frac{\zeta^2}{2}\ell^2-\xi_p\left(\frac{\ell^3}{3}-\zeta\ell^2+\zeta^2\ell\right)\right]. \tag{48}$$

The exact results is the following:

$$m=\frac{\frac{2}{3}Rg_1 I_1-1}{I_2}. \tag{49}$$

For the limiting case, where $\ell\gg\zeta,\xi_p$, the dominant terms are those of higher order on ℓ, whose integral is separated as:

$$I_1\sim\frac{\ell^3}{12s},\qquad I_2\sim\frac{\ell^4}{16s}. \tag{50}$$

The asymptotic behavior is given by

$$m\approx\frac{4}{9}\frac{Rg_1}{\ell}. \tag{51}$$

Data availability

No data was used for the research described in the article.

References

[1] Fisher RA. The wave of advance of advantageous genes. Ann Eugen 1937;7:355–69.
[2] Kolmogorov AN, Petrovskii IG, Piskunov NS. Study of the diffusion equation with growth of the quantity of matter and its application to a biological problem. Mosc Univ Math Bull 1937;1:1–25.
[3] Curilef S. Derivation and analytical solutions of a non-linear diffusion equation applied to non-constant heat conductivity and ionic diffusion in glasses. Chaos 2022;32:113133.
[4] Curilef S, Plastino AR, Curado EMF. Multi-dimensional q-Gaussian densities describing systems of confined interacting particles with drag. Eur Phys J Plus 2025;140:39.
[5] Curilef S, Plastino AR, Wedemann RS. Statistical dynamics of driven systems of confined interacting particles in the overdamped-motion regime. Chaos 2022;32:113134.
[6] Curilef S, González D, Calderón C. Analyzing the 2019 Chilean social outbreak: Modelling Latin American economies. PLoS One 2021;16:e0256037.
[7] Valenzuela C, del Pino LA, Curilef S. Analytical solutions for a non-linear diffusion equation with convection and reaction. Phys A 2014;416:439–51.
[8] Troncoso P, Fierro O, Curilef S, Plastino AR. A family of evolution equations with non-linear diffusion, verhulst growth, and global regulation: Exact time-dependent solutions. Phys A 2007;375:457–66.
[9] Prozorov AA, Trifonov AYu, Shapovalov AV. Asymptotic behavior of the one-dimensional Fisher–Kolmogorov–Petrovskii–Piskunov equation with anomalous diffusion. Russ Phys J 2015;58:399–409.
[10] Li P, Wang Q, Xu C, Tian D, Li P. Fractional analysis of a coupled dual-capacitance neuronal model with state-wise surrogate neural networks. Neural Netw 2026;204:109257.
[11] Li P, Qiao R, Farman M, Xu C, Yao M, Nisar KS, Qu Y. Investigation the epidemiological transition of Ebola virus under contagious population with sustainable extended fractional operator. Math Biosci 2026;397:109693.

[12] Kevrekidis IG, Gear CW, Hummer G. Equation-free: The computer-aided analysis of complex multiscale systems. AIChE J 2004;50:1346–55.
[13] Holmes P, Lumley JL, Berkooz G, Rowley CW. Turbulence, coherent structures, dynamical systems and symmetry. second ed. Cambridge: Cambridge University Press; 2012.
[14] Goodman RH. Chaotic scattering in solitary wave interactions: A singular iterated-map description. Chaos 2008;18:023113.
[15] Kaup DJ, Malomed BA. The variational principle for nonlinear waves in dissipative systems. Phys D 1995;87:155–9.
[16] Anderson D. Variational approach to nonlinear pulse propagation in optical fibers. Phys Rev A 1983;27:3135–45.
[17] Murray JD. Mathematical biology: I. an introduction. 3rd ed. New York: Springer; 2002.
[18] Plastino AR, Plastino A. Non-extensive statistical mechanics and generalized Fokker–Planck equation. Phys A 1995;222:347–54.
[19] Frank TD. Nonlinear Fokker–Planck equations: fundamentals and applications. Berlin: Springer; 2005.
[20] Tsallis C, Bukman DJ. Anomalous diffusion in the presence of external forces: Exact time-dependent solutions and their thermostatistical basis. Phys Rev E 1996;54:R2197–200.
[21] Wiggins S. Introduction to applied nonlinear dynamical systems and chaos. 2nd ed. New York: Springer; 2003.
[22] Carr J. Applications of centre manifold theory. New York: Springer; 1981.
[23] Kenmogne F, Yemélé D, Kengne J, Ndjanfang D. Transverse compactlike pulse signals in a two-dimensional nonlinear electrical network. Phys Rev E 2014;90:052921.
[24] Gonpe Tafo JB, Kenmogne F, Mando Kongne A, Eno R, Yemélé D. Modulated solitons and transverse stability in a two-dimensional nonlinear reaction–diffusion electrical network. Results Phys 2023;50:106532.
[25] Mabou WK, Ndjanfang D, Nfor NO, Andrew MF, Kenmogne F, Donkeng HY, Yemélé D. Dynamics of nonlinear waves in a low-pass reaction–diffusion electrical network and some exact and implicit modulated compact solutions. Phys D 2025;472:134532.
[26] Newman TJ, Kolomeisky EB, Antonovics J. Population dynamics with global regulation: The conserved Fisher equation. Phys Rev Lett 2004;92:228103.
[27] Briguglio L, Cordina G, Farrugia N, Vella S. Economic vulnerability and resilience: Concepts and measurements. Oxf Dev Stud 2009;37:229–47.
[28] Schluter C. Top incomes, heavy tails, and rank–size regressions. Econometrics 2018;6:10.
[29] Delhey J, Dragolov G. Why inequality makes Europeans less happy: The role of distrust, status anxiety, and perceived conflict. Eur Sociol Rev 2014;30:151–65.